

## Chiral metamaterials: simulations and experiments

This article has been downloaded from IOPscience. Please scroll down to see the full text article.

2009 J. Opt. A: Pure Appl. Opt. 11 114003

(<http://iopscience.iop.org/1464-4258/11/11/114003>)

[The Table of Contents](#) and [more related content](#) is available

Download details:

IP Address: 139.91.179.8

The article was downloaded on 10/11/2009 at 12:27

Please note that [terms and conditions apply](#).

## REVIEW ARTICLE

# Chiral metamaterials: simulations and experiments

Bingnan Wang<sup>1</sup>, Jiangfeng Zhou<sup>1</sup>, Thomas Koschny<sup>1,2,3</sup>,  
Maria Kafesaki<sup>2,3</sup> and Costas M Soukoulis<sup>1,2,3</sup>

<sup>1</sup> Ames Laboratory and Department of Physics and Astronomy, Iowa State University, Ames, IA 50011, USA

<sup>2</sup> Institute of Electronic Structure and Laser, FORTH, Heraklion, Crete, 71110, Greece

<sup>3</sup> Department of Materials Science and Technology, University of Crete, Heraklion, Crete, 71110, Greece

E-mail: [soukoulis@ameslab.gov](mailto:soukoulis@ameslab.gov)

Received 20 February 2009, accepted for publication 6 May 2009

Published 16 September 2009

Online at [stacks.iop.org/JOptA/11/114003](http://stacks.iop.org/JOptA/11/114003)

## Abstract

Electromagnetic metamaterials are composed of periodically arranged artificial structures. They show peculiar properties, such as negative refraction and super-lensing, which are not seen in natural materials. The conventional metamaterials require both negative  $\epsilon$  and negative  $\mu$  to achieve negative refraction. Chiral metamaterial is a new class of metamaterials offering a simpler route to negative refraction. In this paper, we briefly review the history of metamaterials and the developments on chiral metamaterials. We study the wave propagation properties in chiral metamaterials and show that negative refraction can be realized in chiral metamaterials with a strong chirality, with neither  $\epsilon$  nor  $\mu$  negative required. We have developed a retrieval procedure, adopting a uniaxial bi-isotropic model to calculate the effective parameters such as  $n_{\pm}$ ,  $\kappa$ ,  $\epsilon$  and  $\mu$  of the chiral metamaterials. Our work on the design, numerical calculations and experimental measurements of chiral metamaterials is introduced. Strong chiral behaviors such as optical activity and circular dichroism are observed and negative refraction is obtained for circularly polarized waves in these chiral metamaterials. We show that 3D isotropic chiral metamaterials can eventually be realized.

**Keywords:** metamaterials, chirality, optical activity, negative refraction

(Some figures in this article are in colour only in the electronic version)

## 1. Introduction

### 1.1. Metamaterial and negative refraction

Electromagnetic metamaterials are periodically arranged artificial structures that show peculiar properties, such as negative refraction, which are not seen in natural materials (for reviews of the metamaterial field, see [1–3]). The elemental structures of the metamaterials are typically much smaller in size relative to the wavelength such that the metamaterials can be considered as homogeneous. Macroscopic parameters such as electric permittivity  $\epsilon$  and magnetic permeability  $\mu$  can then be used to describe the electromagnetic (EM) properties

of the metamaterials [4]. The fascinating, but challenging work of scientists and engineers in this area is to design new structures, or photonic atoms, to achieve the EM properties of metamaterials they desire for specific applications.

To realize negative refraction in metamaterials, both  $\epsilon$  and  $\mu$  need to be negative [5]. The negative  $\epsilon$  can be achieved with an array of long and thin metallic wires, serving as electric resonators. Just like the electric plasmonic behavior of metals, the  $\epsilon$  of the medium is negative below the effective plasma frequency. By adjusting the geometry of the wires and the distance between wires, the plasma frequency can be scaled down to the microwave region. The negative  $\mu$  is first realized by the so-called split-ring resonator (SRR) structure, proposed

by Pendry *et al* [4]. The SRRs are composed of metallic rings with gaps. Although made of non-magnetic materials, the SRRs are magnetically active and can give strong responses to magnetic fields. By tuning the geometric parameters of SRRs, a band of negative  $\mu$  can be obtained at the desired frequency range. If designed properly, the combination of these two sets of resonators can give both negative  $\epsilon$  and negative  $\mu$  in the same frequency band. This is realized with microwave experiments by Smith *et al* [6] in 2000. The same group further demonstrated negative refraction by measuring the output signal of EM waves refracted by a metamaterial in a wedge shape [7]. Since then, the SRR and metallic wire structures were studied extensively by research groups all over the world, both theoretically and experimentally. Applications of metamaterials, such as super-lens [1, 8], and invisible cloaks [9, 10], were proposed and studied.

By scaling down the SRR size and simplifying the structure, magnetic metamaterials were fabricated to show magnetic responses from the THz to infrared region [11–14]. However, the scaling rule breaks down beyond 200 THz, due to the fact that metals cannot be considered as perfect conductors anymore [15]. Another disadvantage is that, for the SRR structures, the magnetic field needs to be perpendicular to the plane to obtain the magnetic resonance. Normal incidence of EM waves to the planar SRR structures does not excite directly the magnetic resonance. Plus, the SRR and wire combination is too complicated to be fabricated in nanoscale, especially when a three-dimensional (3D) medium is needed.

New designs were proposed to achieve negative refraction towards the optical regime [16–19]. Unlike the SRRs, these new designs are typically layered structures, with a dielectric substrate in the middle. The two metal layers on each side of the substrate are identical and composed of short wires, metal plates or fishnet-like structures. While the parallel dipole resonance in each metal structure gives negative  $\epsilon$ , the negative  $\mu$  is provided by the antiparallel resonance in the metal structure pairs separated by the substrate. So normal incidence of EM waves is supported. Bulk media can be fabricated by stacking the layered structures. Recently, negative refraction is demonstrated at optical frequencies with stacked fishnet-like structures [20, 21].

On the other hand, another type of metamaterial, the so-called indefinite metamaterials, has also been studied. In contrast to isotropic metamaterials, whose  $\epsilon$  and  $\mu$  are the same in all directions, an indefinite medium has anisotropic  $\epsilon$  and  $\mu$  tensors, with some components having an opposite sign to the rest. In 2001, Lindell *et al* [22] showed that some indefinite media can support backward waves. Smith and colleagues [23, 24] then analyzed the EM wave propagating properties of indefinite media in detail [23] and showed that some types of indefinite media can have the same negative refraction effect as isotropic metamaterials. Partial focusing of a point source by an indefinite medium slab was also described. The wire medium, which is composed of metal wire arrays, is an important medium of this kind. The wire medium is anisotropic and has a negative  $\epsilon$  along the direction of the wires below the plasma frequency. The optical response of such a wire medium is not limited to

resonances, so that the medium has a higher tolerance to fabrication defects and the loss is smaller than in strongly resonant structures [25, 26]. Moreover, the wire array does not even have to be periodic. Subwavelength imaging and negative refraction of the wire medium in infrared and optical frequencies was studied theoretically and numerically [25, 26]. Recently, optical negative refraction has been demonstrated experimentally with silver nanowires [27].

## 1.2. Chiral metamaterials

A chiral medium is composed of particles that cannot be superimposed on their mirror images [28]. A chiral medium has different responses for a left circularly polarized (LCP) wave and a right circularly polarized (RCP) wave due to the intrinsic chiral asymmetry of the medium. Also, there is cross-coupling between the electric field and magnetic field going through a chiral medium. A dimensionless chirality parameter  $\kappa$  is used to describe this cross-coupling effect. The refractive indices of RCP and LCP waves become different due to the existence of  $\kappa$ . These will be explained in detail in the following sections.

There is a long history in the study of chiral media. In the early 19th century, the optical rotation in quartz crystals as well as some liquids and gases had already been discovered by Biot and others [29]. Biot also suggested that the phenomenon has a root in the molecules. The handedness nature of the molecules in optically active materials was confirmed by Pasteur in the 1840s [28]. The discoveries turned out to be useful in areas such as analytical chemistry and pharmaceuticals. In 1873, Lord Kelvin first used the word ‘chirality’ to describe the handedness in his lectures [30]. In the 1910s Lindeman managed to introduce the optical activity phenomenon in visible light to radio waves, with a collection of helical coils serving as artificial chiral ‘molecules’ [28]. The studies of chiral media in the microwave region have found applications in many areas such as antennas, polarizers and waveguides [31].

In 2003, Tretyakov *et al* [32] discussed the possibility of realizing negative refraction by chiral nihility. The authors first proposed the idea to fabricate a metamaterial composed of chiral particles, such as helical wires. To get negative refraction for one of the circular polarizations,  $\kappa$  needs to be larger than  $\sqrt{\epsilon\mu}$ . In natural materials such as quartz and sugar solutions,  $\kappa$  is generally much smaller than 1, while  $\sqrt{\epsilon\mu}$  is generally larger than 1. So negative refraction is not possible in natural chiral materials. However, with chiral metamaterials, the macroscopic parameters can be designed. The idea of chiral nihility is that, when  $\epsilon$  and  $\mu$  of a chiral medium are small and very close to zero, the chirality can make the refractive index for one circular polarization to become negative, even when  $\kappa$  is small.

The metamaterial based on chiral nihility is a special case of chiral metamaterials. In 2004, Pendry [33] discussed in general the possibility to achieve negative refraction in chiral metamaterials. He analyzed the conditions to realize negative refraction in chiral metamaterials and showed that they are simpler than for regular metamaterials, which require

both electric and magnetic resonances to have negative  $\epsilon$  and negative  $\mu$ . In chiral metamaterials, neither  $\epsilon$  nor  $\mu$  needs to be negative. As long as the chiral parameter  $\kappa$  is large enough, negative refraction can be obtained in chiral metamaterials. Pendry then proposed a practical model of a chiral metamaterial working in the microwave regime with twisted Swiss rolls as elemental structures.

## 2. Wave propagation in chiral media

Chiral media belong to a wider range of bi-isotropic (BI) media. BI media [28] are characterized by the following constitutive relations:

$$\mathbf{D} = \epsilon_0 \epsilon \mathbf{E} + (\chi + i\kappa) \sqrt{\mu_0 \epsilon_0} \mathbf{H} \quad (1)$$

$$\mathbf{B} = \mu_0 \mu \mathbf{H} + (\chi - i\kappa) \sqrt{\mu_0 \epsilon_0} \mathbf{E} \quad (2)$$

where  $\epsilon$  is the relative permittivity of the medium,  $\epsilon_0$  is the permittivity of vacuum,  $\mu$  is the relative permeability of the medium and  $\mu_0$  is the permeability of vacuum. The difference between BI media and regular isotropic media lies in the extra terms of the constitutive relations.  $\chi$  is the dimensionless magneto-electric parameter and describes the reciprocity of the material. Materials with  $\chi \neq 0$  are non-reciprocal.  $\kappa$  is the dimensionless chirality parameter of the material. Materials with  $\kappa \neq 0$  are chiral. The imaginary unit  $i$  in the formula is from the time-harmonic convention  $e^{-i\omega t}$ .

Depending on the values of  $\chi$  and  $\kappa$ , the BI media can be classified as

- General BI medium: non-reciprocal ( $\chi \neq 0$ ), chiral ( $\kappa \neq 0$ );
- Tellegen medium: non-reciprocal ( $\chi \neq 0$ ), non-chiral ( $\kappa = 0$ );
- Pasteur medium: reciprocal ( $\chi = 0$ ), chiral ( $\kappa \neq 0$ ).

We are interested in the Pasteur medium, or the reciprocal chiral medium.

Consider the plane wave propagation in an isotropic chiral medium. Combining the above constitutive relations with  $\chi = 0$  and the frequency-domain source-free Maxwell's equations, the following wave equation can be obtained for the electric field  $\mathbf{E}$ :

$$\mathbf{k} \times (\mathbf{k} \times \mathbf{E}) = -k_0^2 (\epsilon \mu - \kappa^2) \mathbf{E} - 2i\kappa k_0 (\mathbf{k} \times \mathbf{E}) \quad (3)$$

where  $\mathbf{k}$  is the wavevector in the chiral medium,  $k_0 = \omega/c$  is the free-space wavevector and  $c = \sqrt{\epsilon_0 \mu_0}$  is the speed of light in vacuum.

For simplicity, and without loss of generality, we assume  $\mathbf{k} = k\hat{z}$ . Then the wave equation is simplified and  $k$  is solved:

$$k_{\pm} = k_0 (n \pm \kappa) \quad (4)$$

where  $n = \sqrt{\epsilon \mu}$  is the index of refraction of the medium without chirality. From this equation we can write the chiral parameter  $\kappa$  as  $\kappa = \frac{k_+ - k_-}{2k_0}$ .

The eigenvectors, or the allowed solutions of plane waves in the chiral medium, can then be obtained from  $\mathbf{E}(\mathbf{r}) = (E_{0x}\hat{x} + E_{0y}\hat{y})e^{ikz}$ . Then we get the following relations:

$$\frac{E_{0y}}{E_{0x}} = \frac{k_0^2 (n^2 - \kappa^2) - k_{\pm}^2}{2ik_0 \kappa k_{\pm}} = \pm i. \quad (5)$$

So, the wavevector solution  $k_+$  corresponds to the eigenvector of the RCP wave and  $k_-$  corresponds to the eigenvector of the LCP wave. Here the handedness is defined as seen from the source, or as looking in the direction of propagation. Define the index of refraction of RCP/LCP waves as  $n_{\pm}$ : then from the relation  $k_{\pm} = n_{\pm} k_0$ , we can get

$$n_{\pm} = n \pm \kappa. \quad (6)$$

The polarization plane of a linearly polarized light will rotate when it passes through a chiral medium. This polarization effect is called optical activity and is characterized by the polarization azimuth rotation angle of elliptically polarized light:

$$\theta = \frac{1}{2} \delta = \frac{1}{2} [\arg(T_{++}) - \arg(T_{--})]. \quad (7)$$

The first subscript in  $T_{++}$  and  $T_{--}$  indicates the initial polarization and the second subscript indicates the transmitted polarization. So  $T_{++}$  and  $T_{--}$  are the transmission coefficients for RCP and LCP waves, respectively.

Due to the chiral nature of the medium and the circularly polarized waves, the LCP and RCP light interacts with the particles of the chiral medium differently. This causes the difference in absorption and distortion of the two polarizations going through the medium, which is called circular dichroism. Since the impedance of the chiral medium is the same for the two different polarizations, the reflections of the two polarizations are the same. Then the circular dichroism is characterized by the ellipticity, which is defined from the difference in transmitted power of the two polarizations:

$$\eta = \frac{1}{2} \sin^{-1} \left( \frac{|T_{++}|^2 - |T_{--}|^2}{|T_{++}|^2 + |T_{--}|^2} \right). \quad (8)$$

## 3. Parameter retrieval of chiral media

In the study of metamaterials, parameter retrieval is an important technique to characterize the EM properties of the effective media and is used extensively by researchers, with both numerical and experimental methods to guide the design of new metamaterials and identify the negative refractive behavior of metamaterials.

Parameter retrieval is the procedure of obtaining the macroscopic parameters of a medium based on the transmission and reflection coefficients ( $S$  parameters) from a planar slab of this medium. For a homogeneous material,  $\epsilon$ ,  $\mu$  and the refractive index  $n$  are intrinsic properties of the material and are irrelevant to the thickness of the slab. Thus one can choose a slab as thin as possible to do the measurements, and thus obtain the parameters without ambiguity. However, for a metamaterial slab, the structures are inhomogeneous and

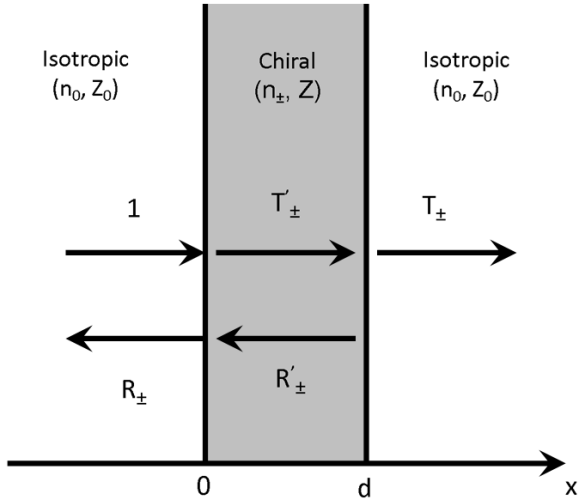


**Figure 1.** The transmission and reflection coefficients of a plane wave incident upon a chiral slab from the left.

the smallest slab thickness is limited by the unit cell size of the metamaterial [34–36]. The retrieval solution in this case is generally multi-branched. The branches need to be chosen carefully to obey energy conservation rules.

For a chiral slab, the retrieval process is generally the same as regular metamaterials, but a little more complicated. The refractive indices for the two eigensolutions (RCP and LCP waves) need to be calculated [37]. Consider a circularly polarized plane wave normally incident upon a homogeneous one-dimensional (1D) chiral slab of thickness  $d$  in vacuum, with refractive index  $n_{\pm}$  and impedance  $Z$  for RCP/LCP waves (see figure 1). The incident wavevector  $k_0$  is in the  $z$  direction and the wavevector in the chiral slab for the RCP/LCP wave is  $k_{\pm}$ . The electric and magnetic field vectors are all tangential to the interfaces in this scenario.

Suppose the incident RCP/LCP electric field has unit amplitude, the reflection coefficient is given by  $R_{\pm}$  and the transmission coefficient after the second interface is given by  $T_{\pm}$ . Multireflection happens inside the chiral slab and the transmitting and reflecting waves inside the chiral slab are represented by coefficients  $T'_{\pm}$  and  $R'_{\pm}$  for RCP and LCP waves (see figure 1). Note that the polarization state is reversed after reflection. Define normalized impedance of the chiral slab as  $z = Z/Z_0$ , where  $Z_0 = \sqrt{\mu_0/\epsilon_0}$  is the free-space impedance.

The tangential electric field and magnetic field are continuous at the first interface ( $x = 0$ ):

$$1 + R_{\pm} = T'_{\pm} + R'_{\pm} \quad (9)$$

$$1 - R_{\pm} = \frac{T'_{\pm} - R'_{\pm}}{z}. \quad (10)$$

Similarly at the second interface ( $x = d$ ):

$$T'_{\pm}e^{ik_{\pm}d} + R'_{\pm}e^{-ik_{\pm}d} = T_{\pm} \quad (11)$$

$$\frac{T'_{\pm}e^{ik_{\pm}d} - R'_{\pm}e^{-ik_{\pm}d}}{z} = T_{\pm}. \quad (12)$$

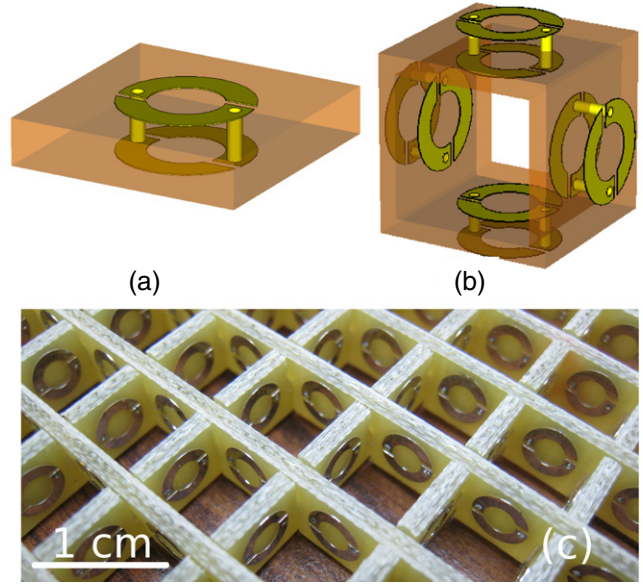


**Figure 2.** (a) The structure of the chiral SRR. (b) A unit cell of the 2D chiral metamaterial. (c) A photo of the fabricated chiral metamaterial. (Adapted from [44].)

Note that  $k_+ + k_- = 2nk_0$ , we can get the transmission and reflection coefficients from the above equations:

$$T_{\pm} = \frac{4ze^{ik_{\pm}d}}{(1+z)^2 - (1-z)^2e^{2ink_0d}} \quad (13)$$

$$R_{\pm} = \frac{(1-z^2)(e^{2ink_0d} - 1)}{(1+z)^2 - (1-z)^2e^{2ink_0d}}. \quad (14)$$

$R_+$  and  $R_-$  are equal since the impedance for RCP and LCP waves is the same. If we denote  $T$  and  $R$  as the transmission and reflection coefficients for the  $\kappa = 0$  medium, we have

$$R_{\pm} = R \quad (15)$$

$$T_{\pm} = Te^{\pm ik_0d}. \quad (16)$$

The impedance and refractive index can be calculated from the above coefficients:

$$z = \pm \sqrt{\frac{(1+R)^2 - T_+T_-}{(1-R)^2 - T_+T_-}} \quad (17)$$

$$n_{\pm} = \frac{i}{k_0d} \left\{ \log \left[ \frac{1}{T_{\pm}} \left( 1 - \frac{z-1}{z+1} R \right) \right] \pm 2m\pi \right\} \quad (18)$$

where  $m$  can be any integer.

The sign of the square root in equation (17) and the multi-branches in equation (18) need to be chosen carefully according to the energy conservation principle, i.e. the real part of impedance  $z$  must be positive, as well as the imaginary part of  $n$ .

Once  $z$  and  $n_{\pm}$  are fixed, the other parameters can be identified subsequently.  $\kappa = (n_+ - n_-)/2$ ,  $n = (n_+ + n_-)/2$ ,  $\mu = nz$  and  $\epsilon = n/z$ .

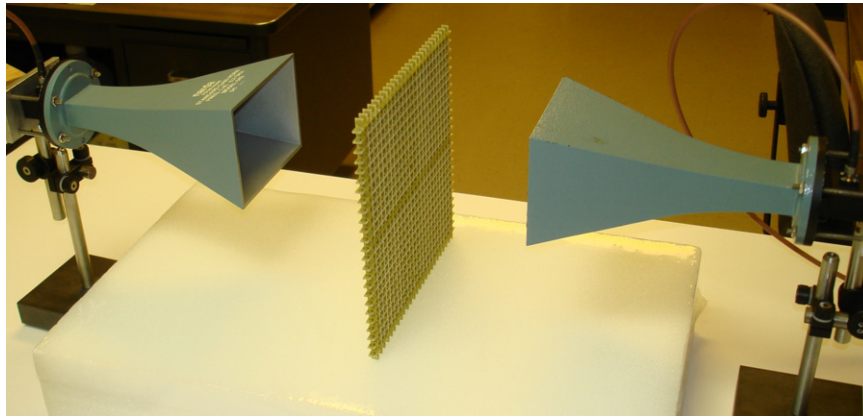


**Figure 3.** The transmission and reflection coefficients of the chiral metamaterial slab is measured by a pair of horn antennas serving as transmitter and receiver. The cables on the horn antennas are connected to a vector network analyzer (not shown).

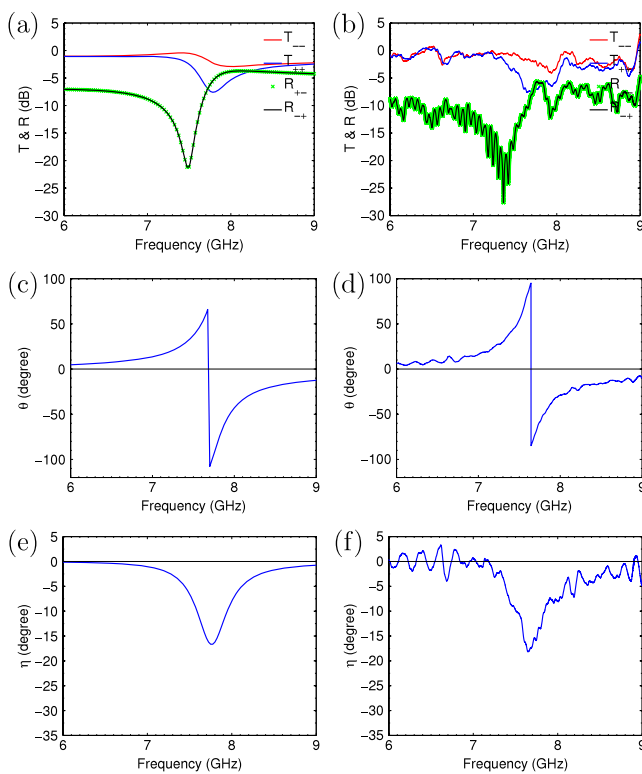


**Figure 4.** From top to bottom, the transmission and reflection amplitudes for LCP and RCP waves, the azimuth rotation angle for linearly polarized waves, and the ellipticity. Simulation results are shown on the left and experiment results are shown on the right. (Adapted from [44].)

#### 4. Work on chiral metamaterials

The research efforts on chiral metamaterials, since the idea was first proposed [32, 33], have moved forward in two directions: bulk chiral metamaterials and planar chiral thin films.

##### 4.1. Studies on 3D chiral metamaterials

The idea of making use of helical inclusions in the pioneering work of Tretyakov *et al* [32] was further studied [38]. A

theoretical model of helical inclusions as building blocks of bulk chiral metamaterial was proposed. The possibilities of negative refraction and ‘perfect lensing’ [8] were discussed. Later on, the idea of building a bulk chiral metamaterial with a negative index of refraction, by manipulating the parameters of the helical inclusions, was discussed [39]. The refractive properties of uniaxially anisotropic chiral media composed of helices were studied theoretically [40]. The conditions to obtain negative refraction were shown to be easier in chiral metamaterials than in regular metamaterials. So far, most of the studies on bulk chiral metamaterials based on helical inclusions are theoretical. No experimental result on bulk chiral metamaterials has been reported yet. This is partly due to the difficulty in the fabrication and homogenization of 3D structures.

In 2007, Marqués *et al* [41] proposed a quasi-planar version of helices, which can be easily fabricated on printed circuit boards (PCB). This quasi-planar chiral structure is a chiral variant of SRRs, which is formed by two identical SRRs separated by a dielectric substrate and interconnected by vias, see figure 2(a). The design of bulk isotropic magnetic metamaterials based on SRRs was discussed [42]. It was shown that resonators satisfying the tetrahedral group of symmetry, arranged in cubic Bravais lattices, are enough to provide isotropy in 3D. Several different resonators based on SRRs were analyzed and very good isotropy was shown by microwave experimental measurements.

Based on the work of [42] and [41], Jelinek *et al* proposed an idea to develop 3D, isotropic chiral metamaterials [43]. By arranging the chiral SRRs in cubic (fcc) Bravais lattices, a BI medium can be obtained. By calculating the susceptibility parameters, including the chiral parameter  $\kappa$ , by Lorentz local field theory, the medium was shown to provide negative refraction over a frequency band.

Recently, a non-planar metamaterial slab made of chiral SRRs has been fabricated and studied by our group [44]. Strong optical activity, circular dichroism, as well as negative refraction, have been demonstrated by both numerical calculations and experimental measurements. This is an important step toward the design and characterization of 3D isotropic chiral metamaterials.

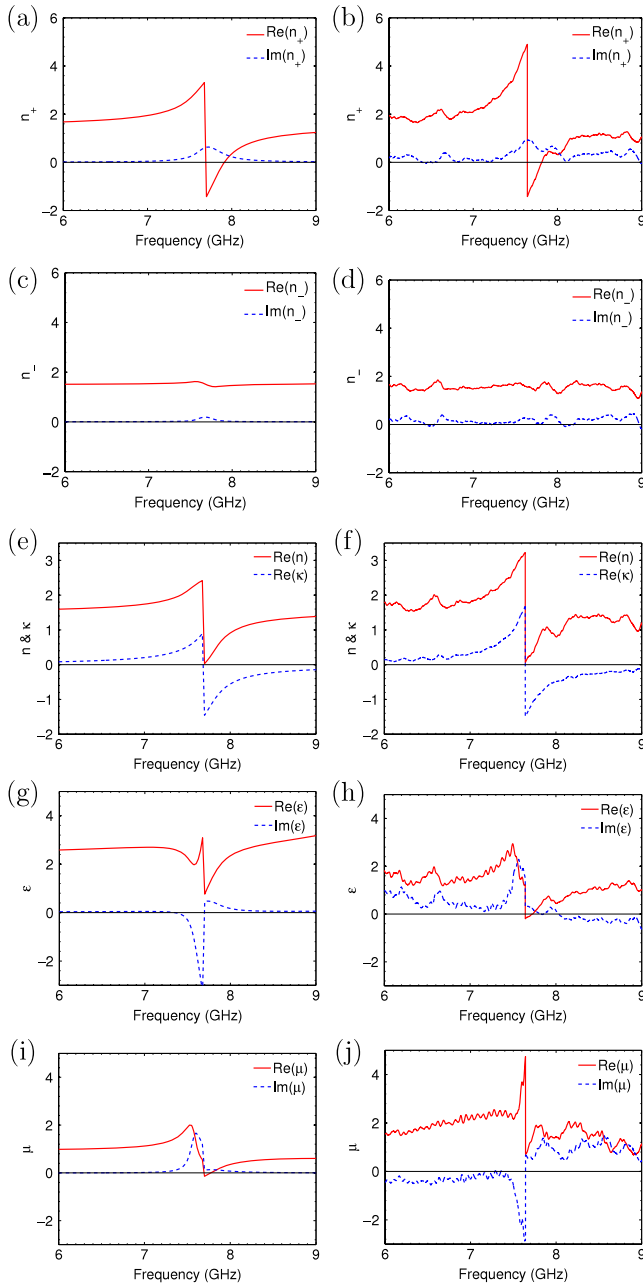


**Figure 5.** The retrieved effective parameters of the chiral metamaterial. The figures from top to bottom are the index of refraction for the two circularly polarized waves  $n_+$  and  $n_-$ , the effective index of refraction  $n$  together with the chiral parameter  $\kappa$ , the effective relative permittivity  $\epsilon$  and relative permeability  $\mu$ . Simulation results are shown on the left and experimental results are shown on the right. (Adapted from [44].)

The chiral structures are fabricated on the two sides of FR-4 printed circuit boards (PCBs), with relative dielectric constant  $\epsilon_r = 3.76$ , loss tangent 0.0186 and thickness 1.6 mm. The metal structures are built with copper 36  $\mu\text{m}$  thick. The SRRs are two-gap split rings with an identical gap width of 0.3 mm. The inner radius of the rings is 1.25 mm and the outer radius is 2.25 mm. The SRRs on opposite sides of the board are connected by vias with a diameter of 0.5 mm. The distance between adjacent rings is 8 mm. The sample is fabricated by 50 strips with 26 cells each, which are then interlocked to form

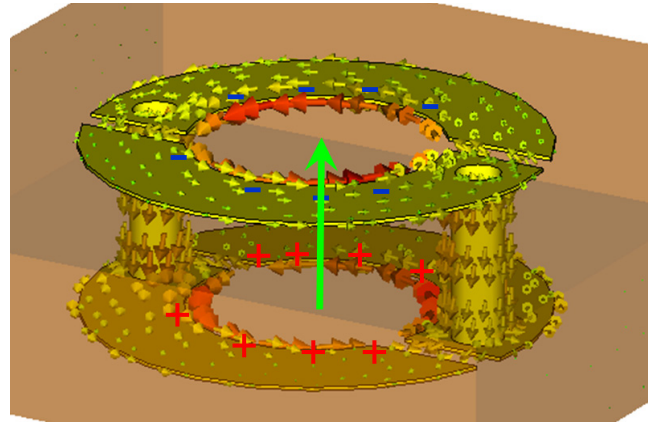


**Figure 6.** The surface current distribution of the SRR near resonance. The circulating current forms a magnetic dipole, causes the opposite charge accumulation on the two SRRs (+ on the bottom SRR and - on the top SRR) and forms an extra electric dipole in the same direction as the magnetic dipole (see green straight arrow). (Adapted from [44].)

a slab of size 208 mm  $\times$  208 mm. Figure 2(b) shows a unit cell of the chiral metamaterial and figure 2(c) presents a picture of the fabricated sample.

The transmission and reflection measurements are done with a vector network analyzer (Agilent E8364B) in our lab. A pair of standard gain horn antennas are used as transmitter and receiver, see figure 3. The signals from these horn antennas are linearly polarized, so the linear transmission coefficients,  $T_{xx}$ ,  $T_{xy}$ ,  $T_{yx}$  and  $T_{yy}$ , are measured, where the first subscript indicates the transmitted field polarization ( $x$ - or  $y$ -polarized) and the second subscript indicates the incident field polarization. The circular transmission coefficients,  $T_{++}$ ,  $T_{+-}$ ,  $T_{-+}$  and  $T_{--}$ , where the first subscript indicates the transmitted field polarization ( $\pm$ , RCP/LCP) and the second subscript indicates the incident field polarization, are converted from the linear transmission coefficients using the following equation:

$$\begin{pmatrix} T_{++} & T_{+-} \\ T_{-+} & T_{--} \end{pmatrix} = \frac{1}{2} \times \begin{pmatrix} (T_{xx} + T_{yy}) + i(T_{xy} - T_{yx}) & (T_{xx} - T_{yy}) - i(T_{xy} + T_{yx}) \\ (T_{xx} - T_{yy}) + i(T_{xy} + T_{yx}) & (T_{xx} + T_{yy}) - i(T_{xy} - T_{yx}) \end{pmatrix}. \quad (19)$$

A similar expression exists for the circular reflection coefficients  $R_{++}$ ,  $R_{+-}$ ,  $R_{-+}$  and  $R_{--}$ .

Figures 4(a) and (b) show the simulated and measured transmission coefficients  $T_{++}$  and  $T_{--}$ , as well as the reflection coefficients  $R_{+-}$  and  $R_{-+}$ , as a function of frequency. The cross-coupling transmission  $T_{-+}$  and  $T_{+-}$  are negligible and they are not shown. An obvious difference (about 5 dB) in  $T_{++}$  and  $T_{--}$  is seen at the resonance frequency 7.7 GHz. The azimuth rotation  $\theta$ , and the ellipticity  $\eta$ , are calculated based on the transmission data and presented in figures 4(c)–(f). At the resonance, the azimuth rotation reaches a maximum of around  $-100^\circ$ . Meanwhile, the ellipticity is also the largest ( $-17^\circ$ ), meaning a linearly polarized wave is strongly distorted and becomes elliptical.

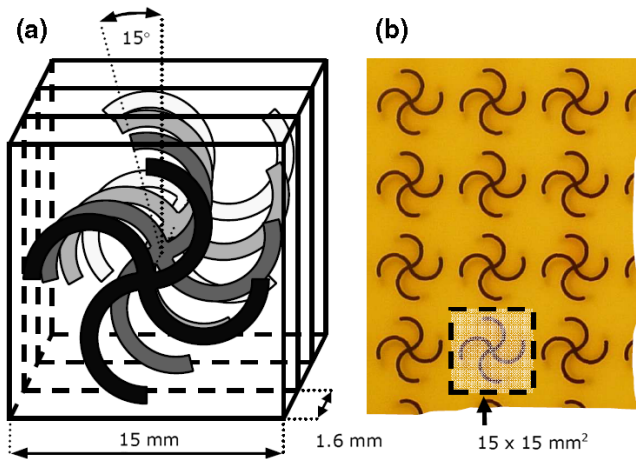


**Figure 7.** Structure of the chiral metamaterial. (a) Schematics of the four-layered metamaterials unit cell. The gammadians in neighboring layers have a relative twist of 15°. The structure of metamaterials with a different number of layers is analogous. (b) Photograph of part of a bi-layered metamaterial sheet. The twisted gammadians of the second layer can be seen as a shaded area thanks to partial transparency to the substrate. A unit cell has been marked. (Adapted from [49].)

The retrieved effective parameters of the chiral metamaterial are shown in figure 5. We see that the effective index of refraction for the RCP wave (figures 5(a) and (b)) shows strong response at resonance and goes negative above the resonance while the index of refraction for the LCP wave (figures 5(c) and (d)) changes only slightly and is positive in all the frequency range. The negative index here is due to a relatively strong chirality  $\kappa$ , and a small value of  $n$  at the resonance (figures 5(e) and (f)). Although there is some discrepancies in simulated and experimental  $\epsilon$  and  $\mu$  (figures 5(g)–(j)), it is obvious that  $\epsilon$  and  $\mu$  are not both negative, which is the signature of conventional negative index metamaterials. The retrieval results show that the negative refraction comes from a strong chirality of the structure, instead of the double-negative ( $\epsilon$  and  $\mu$ ) in conventional metamaterials.

The strong chirality comes from the cross-coupling between electric and magnetic fields going through the

medium. The cross-coupling can be understood by studying the surface current distribution at the resonance (figure 6). Figure 6 shows how an electric dipole is induced by a magnetic field. The incident magnetic field is parallel to the axis of the SRRs and induces circular current around the SRRs, which gives the magnetic dipole. Electric charges with opposite signs (– on the top and + on the bottom SRR) accumulate on the two SRRs, introducing a strong electric dipole (see the green arrow) between the top and bottom SRRs in the same direction as the magnetic dipole. A magnetic dipole can be excited by an electric dipole in a similar manner. This cross-coupling gives the strong chiral parameter of the metamaterial and introduces negative refraction.

As we discussed above, the conditions to get negative refraction in a chiral medium are: small  $\epsilon$  and  $\mu$ , large  $\kappa$  at resonance. Relatively high losses are associated with the strong resonances. New ideas have been proposed to get negative refraction in different ways. Qiu *et al* studied theoretically the wave propagating properties in gyrotropic chiral media, where both  $\epsilon$  and  $\mu$  are described by gyrotropic tensors and  $\kappa$  is described by a scalar [45]. Their study showed that negative refraction can be realized with fewer restrictions and all parameters in the  $\epsilon$  and  $\mu$  tensors, as well as  $\kappa$ , can be positive when negative refraction occurs. The same group also analyzed the behavior of another kind of chiral media, where the chirality parameter  $\kappa$  is describe by a tensor with non-zero off-diagonal elements while  $\epsilon$  and  $\mu$  are described by scalars [46]. The theoretical model showed that negative refraction can be achieved without the requirement of very strong  $\kappa$  due to the gyrotropic parameters.

#### 4.2. Studies on planar chiral metamaterials

On the other hand, research on planar chiral metamaterials has also been reported by many groups, both in theory and experiments [47–53]. Planar structures are easier to fabricate than bulk media and there are very interesting behaviors and potential applications in planar structures, such as strong optical activity and circular dichroism in a thin film. Zheludev and co-workers at the University of Southampton first reported the optical activity of a planar chiral structure with experiments

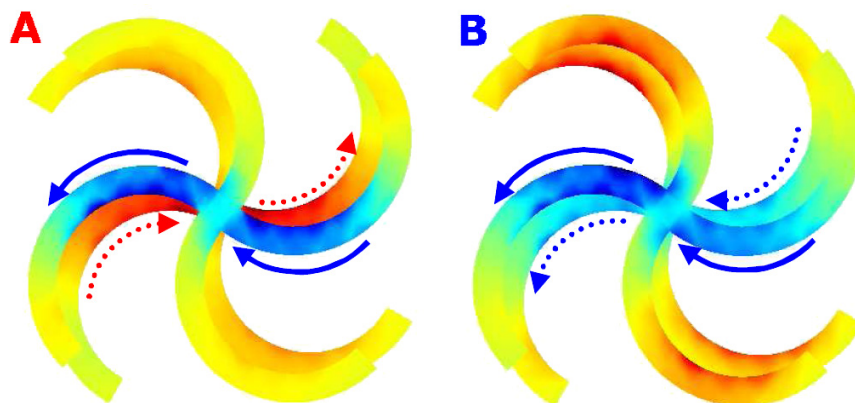


**Figure 8.** Current modes leading to a negative refractive index. The antisymmetric current mode (A) is excited by the RCP wave and the symmetric current mode (B) is excited by the LCP wave. The horizontal component of the excited currents is shown, where blue and red correspond to currents in opposite directions. (Adapted from [49].)

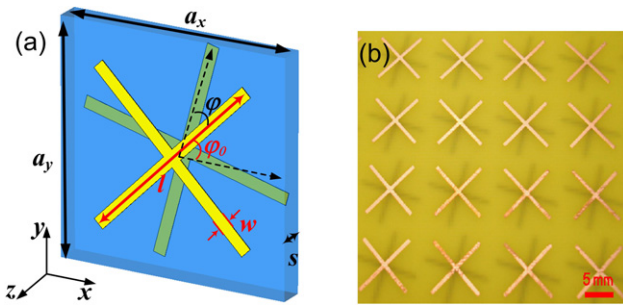


**Figure 9.** (a) Schematic representation of one unit cell of the cross-wire structure. (b) Photograph of one side of a fabricated microwave-scale cross-wire sample. The geometry parameters are given by  $a_x = a_y = 15$  mm,  $l = 14$  mm,  $w = 1$  mm,  $s = 1.6$  mm,  $\phi_0 = 45^\circ$  and  $\phi = 30^\circ$ . (Adapted from [55].)

done in the optical regime [47]. The chiral sample is composed of a single layer of a two-dimensional square array of rosette-shaped wires. The patterns are closely arranged and there is coupling between neighboring patterns. A very large rotation of polarization azimuth (greater than  $30^\circ$ ) is observed. The rotation is found to be associated with both the arrangement of the patterns and the chirality of the pattern itself. Later on, the same group studied a bi-layer rosette-shaped structure (see figures 7 and 8) in the microwave regime [48]. The patterns are physically separated on each layer and the patterns on the second layer are rotated by an angle, instead of identical to the first layer. This turned out to give an extremely strong rotation which, in terms of rotary power per wavelength, is five orders of magnitude larger than a gyrotropic quartz crystal. More recently, this bi-layer structure was proved by experiments to have a negative index of refraction for one of the circularly polarized waves [49].

Meanwhile, the circular dichroism and polarization rotation properties of planar chiral structures, composed of variants of the rosettes, have also been studied by many other groups, both theoretically [50] and experimentally [50–53]. More recently, a negative refractive index of a planar chiral metamaterial, built with arrangements of dual strips connected by a tilted bridge, was demonstrated by parameter retrieval in terahertz frequencies [54].

Actually, the structure on each layer of the bi-layer film does not even have to be chiral to achieve negative refraction. Zhou *et al* [55] recently demonstrated strong rotation of polarization azimuth and negative refraction on a bi-layer structure composed of non-chiral cross-wires.

The layout of the proposed structure is shown in figure 9. A  $18 \times 14$  array of cross-wires is patterned on a double-sided copper-clad FR-4 board. The transmission and reflection coefficients are measured in the same manner as in the chiral SRR experiments. Due to the asymmetric geometry along the propagating direction, the transmission responses for RCP and LCP split into two curves. At the two resonance frequencies of 6.3 and 7.3 GHz, the azimuth rotation and ellipticity reach their maximum values. In the region between two resonance peaks (around 6.9 GHz), which is also the region with low loss and nearly zero dichroism, rotation of polarization can achieve  $-50^\circ$  with  $\eta \approx 0$  [55].

The mechanism of the resonances for the bi-layer rosette and cross-wire pair design can be understood by studying the current density distribution as shown in figures 8 and 10. At the magnetic resonance, the antiparallel current exists on the top and bottom layers (figures 8(a) and 10(a)), which is an asymmetric resonance mode. In figures 8(b) and 10(b), parallel current flows on the two layers, which is a symmetric resonance mode. The current distribution shows that the bi-layer structures can be regarded as a chiral version of the short wire pairs [17, 18, 56], which has the similar current distributions in the symmetric and asymmetric resonance modes.

The chirality of the design comes from the rotation of the second layer of the cross-wires with respect to the first. With an appropriate twist angle, strong chirality can be obtained and the refractive index can go to negative for the RCP wave at one resonance and for the LCP wave at another resonance. When the twist angle is zero, there would be no chiral behavior, even though the resonances can still be seen [55].

## 5. Conclusions

In conclusion, we have briefly reviewed the history of metamaterials, from theoretical proposals to experimental realizations in the GHz, THz and optical regimes. While

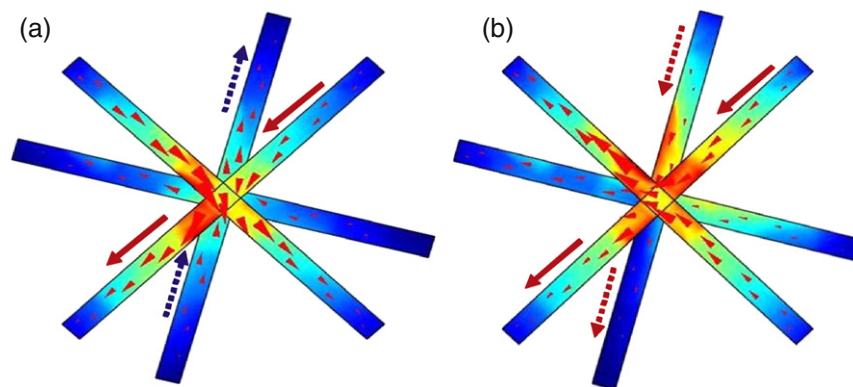


**Figure 10.** The simulated current density distribution for the right circularly polarized EM wave at 6.5 GHz (a) and for the left circularly polarized EM wave at 7.5 GHz (b). (Adapted from [55].)

the conventional metamaterials require negative  $\epsilon$  and  $\mu$  simultaneously to achieve negative refraction, chiral metamaterials offer an alternative and simpler route. We have studied the wave propagation properties in chiral metamaterials and showed that negative refraction can be realized in chiral metamaterials with a strong chirality while neither  $\epsilon$  nor  $\mu$  negative is required. We have developed a retrieval procedure, adopting a uniaxial bi-isotropic model to calculate the effective parameters such as  $n_{\pm}$ ,  $\kappa$ ,  $\epsilon$  and  $\mu$  of the chiral metamaterials. We have reviewed the progress in the chiral metamaterials field, both theoretically and experimentally. We have introduced our new designs, numerical calculations and experimental measurements of chiral metamaterials. We show that very strong chiral behaviors such as optical activity and circular dichroism can be observed. Negative refraction for circularly polarized waves can be obtained with various designs.

## Acknowledgments

Work at Ames Laboratory was supported by the Department of Energy (Basic Energy Sciences) under contract no. DE-AC02-07CH11358. This work was partially supported by the Department of Navy, Office of Naval Research (grant no. N00014-07-1-0359), the European Community FET project PHOME (contract no. 213390) and AFOSR under MURI grant (FA 9550-06-1-0337).

## References

- [1] Smith D R, Pendry J B and Wiltshire M C K 2004 Metamaterials and negative refractive index *Science* **305** 788–92
- [2] Soukoulis C M, Kafesaki M and Economou E N 2006 Negative-index materials: new frontiers in optics *Adv. Mater.* **18** 1941–52
- [3] Soukoulis C M, Linden S and Wegener M 2007 PHYSICS: negative refractive index at optical wavelengths *Science* **315** 47–9
- [4] Pendry J B, Holden A J, Robbins D J and Stewart W J 1999 Magnetism from conductors and enhanced nonlinear phenomena *IEEE Trans. Microw. Theory Tech.* **47** 2075
- [5] Veselago V G 1968 The electrodynamics of substances with simultaneously negative values of  $\epsilon$  and  $\mu$  *Sov. Phys.—Usp.* **10** 509–14
- [6] Smith D R, Padilla W J, Vier D C, Nemat-Nasser S C and Schultz S 2000 Composite medium with simultaneously negative permeability and permittivity *Phys. Rev. Lett.* **84** 4184–7
- [7] Shelby R A, Smith D R and Schultz S 2001 Experimental verification of a negative index of refraction *Science* **292** 77–9
- [8] Pendry J B 2000 Negative refraction makes a perfect lens *Phys. Rev. Lett.* **85** 3966–9
- [9] Pendry J B, Schurig D and Smith D R 2006 Controlling electromagnetic fields *Science* **312** 1780–2
- [10] Schurig D, Mock J J, Justice B J, Cummer S A, Pendry J B, Starr A F and Smith D R 2006 Metamaterial electromagnetic cloak at microwave frequencies *Science* **314** 977–80
- [11] Yen T J, Padilla W J, Fang N, Vier D C, Smith D R, Pendry J B, Basov D N and Zhang X 2004 Terahertz magnetic response from artificial materials *Science* **303** 1494–6
- [12] Linden S, Enkrich C, Wegener M, Zhou J, Koschny T and Soukoulis C M 2004 Magnetic response of metamaterials at 100 Terahertz *Science* **306** 1351–3
- [13] Katsarakis N, Konstantinidis G, Kostopoulos A, Penciu R S, Gundogdu T F, Kafesaki M, Economou E N, Koschny T and Soukoulis C M 2005 Magnetic response of split-ring resonators in the far-infrared frequency regime *Opt. Lett.* **30** 1348–50
- [14] Enkrich C, Wegener M, Linden S, Burger S, Zschiedrich L, Schmidt F, Zhou J F, Koschny T and Soukoulis C M 2005 Magnetic metamaterials at telecommunication and visible frequencies *Phys. Rev. Lett.* **95** 203901
- [15] Zhou J, Koschny T, Kafesaki M, Economou E N, Pendry J B and Soukoulis C M 2005 Saturation of the magnetic response of split-ring resonators at optical frequencies *Phys. Rev. Lett.* **95** 223902
- [16] Zhang S, Fan W, Panoiu N C, Malloy K J, Osgood R M and Brueck S R J 2005 Experimental demonstration of near-infrared negative-index metamaterials *Phys. Rev. Lett.* **95** 137404
- [17] Dolling G, Enkrich C, Wegener M, Zhou J F, Soukoulis C M and Linden S 2005 Cut-wire pairs and plate pairs as magnetic atoms for optical metamaterials *Opt. Lett.* **30** 3198–200
- [18] Shalaev V M, Cai W, Chettiar U K, Yuan H, Sarychev A K, Drachev V P and Kildishev A V 2005 Negative index of refraction in optical metamaterials *Opt. Lett.* **30** 3356–8
- [19] Dolling G, Enkrich C, Wegener M, Soukoulis C M and Linden S 2006 Simultaneous negative phase and group velocity of light in a metamaterial *Science* **312** 892–4
- [20] Dolling G, Wegener M, Soukoulis C M and Linden S 2007 Negative-index metamaterial at 780 nm wavelength *Opt. Lett.* **32** 53–5
- [21] Valentine J, Zhang S, Zentgraf T, Ulin-Avila E, Genov D A, Bartal G and Zhang X 2008 Three-dimensional optical metamaterial with a negative refractive index *Nature* **455** 376–9
- [22] Lindell I V, Tretyakov S A, Nikoskinen K I and Ilvonen S 2001 BW media—media with negative parameters, capable of supporting backward waves *Microw. Opt. Technol. Lett.* **31** 129–33
- [23] Smith D R and Schurig D 2003 Electromagnetic wave propagation in media with indefinite permittivity and permeability tensors *Phys. Rev. Lett.* **90** 077405
- [24] Smith D R, Kolinko P and Schurig D 2004 Negative refraction in indefinite media *J. Opt. Soc. Am. B* **21** 1032–43
- [25] Wangberg R, Elser J, Narimanov E E and Podolskiy V A 2006 Nonmagnetic nanocomposites for optical and infrared negative-refractive-index media *J. Opt. Soc. Am. B* **23** 498–505
- [26] Silveirinha M G, Belov P A and Simovski C R 2007 Subwavelength imaging at infrared frequencies using an array of metallic nanorods *Phys. Rev. B* **75** 035108
- [27] Yao J, Liu Z, Liu Y, Wang Y, Sun C, Bartal G, Stacy A M and Zhang X 2008 Optical negative refraction in bulk metamaterials of nanowires *Science* **321** 930
- [28] Lindell I V, Sihvola A H, Tretyakov S A and Viitanen A J 1994 *Electromagnetic Waves in Chiral and Bi-isotropic Media* (Boston, MA: Artech House Publishers)
- [29] Applequist J 1987 Optical activity: Biot's bequest *Am. Sci.* **75** 58–68
- [30] Barron L D 1982 *Molecular Light Scattering and Optical Activity* (Cambridge: Cambridge University Press)
- [31] Tretyakov S, Serdyukov A, Semchenko I and Sihvola A 2001 *Electromagnetics of Bi-anisotropic Materials: Theory and Applications* (London: Gordon and Breach Science)
- [32] Tretyakov S, Nefedov I, Sihvola A, Maslovski S and Simovski C 2003 Waves and energy in chiral nihility *J. Electromagn. Waves Appl.* **17** 695–706
- [33] Pendry J B 2004 A chiral route to negative refraction *Science* **306** 1353–5

- [34] Smith D R, Schultz S, Markoš P and Soukoulis C M 2002 Determination of effective permittivity and permeability of metamaterials from reflection and transmission coefficients *Phys. Rev. B* **65** 195104
- [35] Smith D R, Vier D C, Koschny T and Soukoulis C M 2005 Electromagnetic parameter retrieval from inhomogeneous metamaterials *Phys. Rev. E* **71** 036617
- [36] Koschny T, Markoš P, Economou E N, Smith D R, Vier D C and Soukoulis C M 2005 Impact of inherent periodic structure on effective medium description of left-handed and related metamaterials *Phys. Rev. B* **71** 245105
- [37] Kwon D, Werner D H, Kildishev A V and Shalaev V M 2008 Material parameter retrieval procedure for general bi-isotropic metamaterials and its application to optical chiral negative-index metamaterial design *Opt. Express* **16** 11822–9
- [38] Tretyakov S, Sihvola A and Jylh L 2005 Backward-wave regime and negative refraction in chiral composites *PECS-VI: 6th Int. Symp. on Photonic and Electromagnetic Crystal Structures; Photon. Nanostruct.—Fundam. Appl.* **3** 107–15
- [39] Semchenko I V, Khakhomov S A and Tretyakov S A 2009 Chiral metamaterial with unit negative refraction index *Eur. Phys. J. Appl. Phys.* **46** 32607
- [40] Cheng Q and Cui T J 2006 Negative refractions in uniaxially anisotropic chiral media *Phys. Rev. B* **73** 113104
- [41] Marqués R, Jelinek L and Mesa F 2007 Negative refraction from balanced quasi-planar chiral inclusions *Microw. Opt. Technol. Lett.* **49** 2606–9
- [42] Baena J D, Jelinek L and Marqués R 2007 Towards a systematic design of isotropic bulk magnetic metamaterials using the cubic point groups of symmetry *Phys. Rev. B* **76** 245115
- [43] Jelinek L, Marqués R, Mesa F and Baena J D 2008 Periodic arrangements of chiral scatterers providing negative refractive index bi-isotropic media *Phys. Rev. B* **77** 205110
- [44] Wang B, Zhou J, Koschny T and Soukoulis C M 2009 Nonplanar chiral metamaterials with negative index *Appl. Phys. Lett.* **94** 151112
- [45] Qiu C, Yao H, Li L, Zouhdi S and Yeo T 2007 Backward waves in magnetoelectrically chiral media: propagation, impedance, and negative refraction *Phys. Rev. B* **75** 155120
- [46] Qiu C, Yao H, Li L, Zouhdi S and Yeo T 2007 Routes to left-handed materials by magnetoelectric couplings *Phys. Rev. B* **75** 245214
- [47] Papakostas A, Potts A, Bagnall D M, Prosvirnin S L, Coles H J and Zheludev N I 2003 Optical manifestations of planar chirality *Phys. Rev. Lett.* **90** 107404
- [48] Rogacheva A V, Fedotov V A, Schwanecke A S and Zheludev N I 2006 Giant gyrotropy due to electromagnetic-field coupling in a bilayered chiral structure *Phys. Rev. Lett.* **97** 177401
- [49] Plum E, Zhou J, Dong J, Fedotov V A, Koschny T, Soukoulis C M and Zheludev N I 2009 Metamaterial with negative index due to chirality *Phys. Rev. B* **79** 035407
- [50] Bai B, Svirko Y, Turunen J and Vallius T 2007 Optical activity in planar chiral metamaterials: theoretical study *Phys. Rev. A* **76** 023811
- [51] Kuwata-Gonokami M, Saito N, Ino Y, Kauranen M, Jefimovs K, Vallius T, Turunen J and Svirko Y 2005 Giant optical activity in quasi-two-dimensional planar nanostructures *Phys. Rev. Lett.* **95** 227401
- [52] Decker M, Klein M W, Wegener M and Linden S 2007 Circular dichroism of planar chiral magnetic metamaterials *Opt. Lett.* **32** 856–8
- [53] Kwon D, Werner P L and Werner D H 2008 Optical planar chiral metamaterial designs for strong circular dichroism and polarization rotation *Opt. Express* **16** 11802–7
- [54] Zhang S, Park Y, Li J, Lu X, Zhang W and Zhang X 2009 Negative refractive index in chiral metamaterials *Phys. Rev. Lett.* **102** 023901
- [55] Zhou J, Dong J, Wang B, Koschny T, Kafesaki M and Soukoulis C M 2009 Negative refractive index due to chirality *Phys. Rev. B* **79** 121104
- [56] Zhou J, Zhang L, Tuttle G, Koschny T and Soukoulis C M 2006 Negative index materials using simple short wire pairs *Phys. Rev. B* **73** 041101